ORGANIC LETTERS

2012
Vol. 14, No. 14
3748–3751

An Indium-Mediated Allylative/ Transesterification DFT-Directed Approach to Chiral $C_{(3)}$-Functionalized Phthalides

Roya Mirabdolbaghi and Travis Dudding*

Department of Chemistry, Brock University, 500 Glenridge Avenue, St. Catharines, Ontario, Canada L2S 3A1

tdudding@brocku.ca

Received June 12, 2012

ABSTRACT

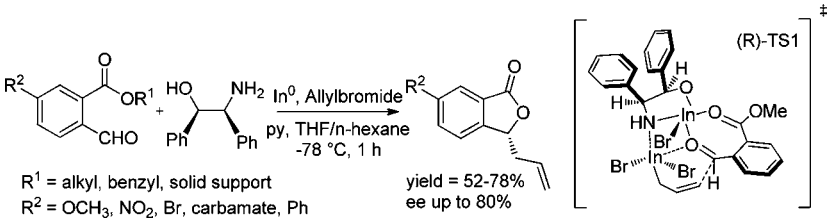

A one-pot synthesis of chiral $C_{(3)}$-substituted phthalides via an indium-mediated allylation/transesterification reaction is described. The development of this reaction was facilitated through the applied use of DFT calculations to rationalize the stereoselection of a chiral In-mediated process. It was discovered that the enantiomeric excess of this reaction depended upon the steric size, chain length, and substitution of the aldehyde employed.

The ability of a catalyst or single reagent to promote a desired cascade of reaction events in a single reaction flask with high enantioselectivity in useful yields represents an efficient strategy for assembling complex synthetic targets, such as natural products. In this context, we were recently attracted by the possibility of employing a chiral indium reagent or catalyst as a resource for preparing optically enriched, value added chemicals and/or synthetic precursors of natural products. Driving this interest was the low toxicity, functional group compatibility, and tolerance to air and moisture of inidium which remains underutilized in synthesis at this time (especially in the field of asymmetric catalysis), apart from a few notable examples.[1−4] To this end, the development of an enantioselective, indium-mediated, synthetic approach to $C_{(3)}$-chiral substituted phthalides, which are a widely distributed structural motif within a number of biologically active natural products and medicinally important pharmaceuticals, appeared an ideal challenge. For instance, the structurally related spirolaxines CJ-12,954 (**1**) and CJ-13,014 (**2**) are reported to lower cholesterol and exhibit cytotoxicity against endothelial (BMEC and Huvec) and tumor (LoVo, HL60) cell lines,[5] while the *Apium* plant seed extract (*S*)-3-*n*-butylphthalide (**3**) has recognized potential as a treatment for stroke and pretreatment for Parkinson's disease (PD) (Figure 1).[6,7]

Given their therapeutic properties, it is perhaps not surprising that a number of efficient synthetic routes to

(1) Hirayama, L. C.; Gamsey, S.; Knueppel, D.; Steiner, D.; DeLaTorre, K.; Singaram, B. *Tetrahedron Lett.* **2005**, *46*, 2315–2318.
(2) Yus, M.; Gonzalez-Gomez, J. C.; Foubelo, F. *Chem. Rev.* **2011**, *111*, 7774–7854.
(3) Kargbo, R. B.; Cook, G. R. *Curr. Org. Chem.* **2007**, *11*, 1287–1309.
(4) Loh, T. P.; Zhou, J. R.; Yin, Z. *Org. Lett.* **1999**, *1*, 1855–1857.

(5) (a) Blaser, M. J. *Clin. Infect. Dis.* **1992**, *15*, 386–393. (b) Bava, A.; Clericuzio, M.; Giannini, G.; Malpezzi, L.; Meille, S. V.; Nasini, G. *Eur. J. Org. Chem.* **2005**, *11*, 2292–2296. (c) Radcliff, F. J.; Fraser, J. D.; Wilson, Z. E.; Heapy, A. M.; Robinson, J. E.; Bryant, C. J.; Flowers, C. L.; Brimble, M. A. *Bioorg. Med. Chem.* **2008**, *16*, 6179–6185.
(6) Xiong, N.; Huang, J.; Chen, C.; Zhao, Y.; Zhang, Z.; Jia, M.; Zhang, Z.; Hou, L.; Yang, H.; Cao, X.; Liang, Z.; Zhang, Y.; Sun, S.; Lin, Z.; Wang, T. *Neurobiol. Aging* **2012**, *33*, 1777–1791.
(7) For more examples see: (a) Robinson, J. E.; Brimble, M. A. *Chem. Commun.* **2005**, 1560–1562. (b) Nannei, R.; Dallavalle, S.; Merlini, L.; Bava, A.; Nasini, G. *J. Org. Chem.* **2006**, *71*, 6277–6280. (c) Keaton, K. A.; Phillips, A. J. *Org. Lett.* **2007**, *9*, 2717–2719. (d) Arnone, A.; Assante, G.; Nasini, G.; Depava, O. V. *Phytochemistry* **1990**, *29*, 613–616. (e) Tianpanich, K.; Prachya, S.; Wiyakrutta, S.; Mahidol, C.; Ruchirawat, S.; Kittakoop, P. *J. Nat. Prod.* **2011**, *74*, 79–81.

10.1021/ol301566f
Published on Web 07/11/2012

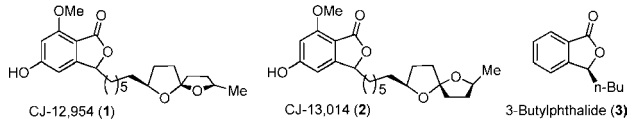

Figure 1. Examples of natural products containing $C_{(3)}$-chiral-substituted phthalides.

optically enriched $C_{(3)}$-chiral phthalides have been reported.[8] Nevertheless, there remains a pressing need for sythetic routes to $C_{(3)}$-chiral phthalides, as the majority of the reported approaches are limited in substrate scope, use expensive and/or toxic rare earth transition metals, and provide low levels of enantioselection.

Fully aware of these limitations, we were drawn toward the possibility of developing a more robust and synthetically efficient strategy for preparing optically enriched $C_{(3)}$-chiral phthalides. Accordingly, we describe here a target-oriented assembly of chiral $C_{(3)}$-substituted phthalides via the orchestrated use of rational forethought (i.e., density functional theory (DFT) calculations) in prelude to experimental practice. Notably, this work has also provided theoretical models for rationalizating the enantioinduction of the reactions, and the ligand component used was easily recoverable after the reaction. This work has led to a revision of the stereochemical assignment of the allylation products reported by Singaram et al. (vide infra).

At the outset of this work, with the goal of developing an In-mediated protocol for preparing $C_{(3)}$-chiral phthalides, we envisioned using a reaction scenario such as that outlined in Scheme 1. In this mechanistic proposal, a highly reactive In-allyl species, **4**, is generated in situ from **3**, inexpensive indium metal, and allyl bromide (step 1). Intermediate **4** then reacts with methyl-2-formylbenzoate **1** (step 2) to give allyl intermediate **5**, which subsequently undergoes a dual In-metal/pyridium salt (pyr-H^+) catalyzed intramolecular transesterification to afford (*R*)-3-allylisobenzofuran-1(3*H*)-one **2** (step 3). However, because of the frequently observed erosion in the enantioseletion of catalytic asymmetric allylations of *ortho*-substituted substrates,[9−11] we were concerned if this process would in fact impart enantioselectivity.[12] For this reason, in keeping with our philosophy of utilizing computation to augment experimental development, we initially turned to DFT calculations to discern to what, if any, extent this process would afford enantioselection. Thus, working under the assumption that allylation was the (*R*)- vs (*S*)-enantioselective-determining step of this reaction, the addition of **4** to **1** was modeled using the Gaussian 09 suite of programs at the B3LYP/LanL2DZ level of theory with the IEFPCM dielectric continuum solvation model and the default parameters for THF (ε = 7.6).

Scheme 1. Envisioned Mechanistic Cycle for the Synthesis of $C_{(3)}$-Substituted Phthalides

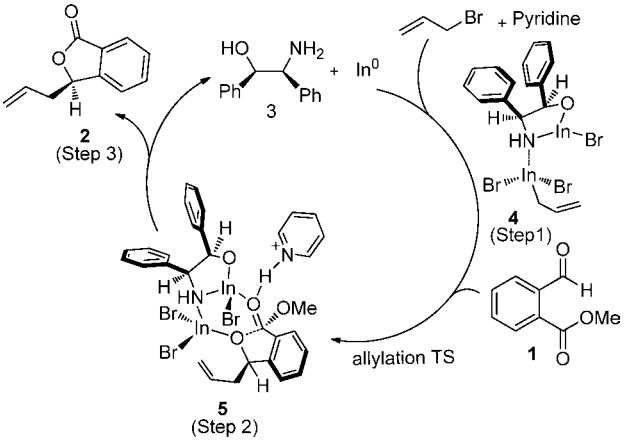

Surfacing from these calculations were a number of insightful features with respect to the first-order saddle points, (*R*)-**TS1** and (*S*)-**TS2**, governing the (*R*)- vs (*S*)-enantioselective allylation (Figure 2). A particularly dominant feature of these transition states was the presence of a bidentate mode of (LUMO-lowering) aldehdye activation by the two In-metal centers ($In_{(1)}\cdots O_{(1)}$ and $In_{(2)}\cdots O_{(1)}$), which interestingly, because of geometric constraints, only occurred in the two lowest transition structures, (*R*)-**TS1** and (*S*)-**TS2**. A second notable feature of these two transition structures is that the $In_{(1)}$-metal center resides within the plane of the 5-membered ring system containing the N- and O-atoms of the ligand, while the $In_{(2)}$-metal center resides below the plane of this same 5-membered ring system and *trans* to the bulky phenyl substituents of the ligand. Geometrically, this in-plane/below the plane relationship of the two In-metals with respect to the sterically bulky vicinal phenyl groups of the ligand component in (*R*)-**TS1** and (*S*)-**TS2** shields the top face of these structures, forcing allylation to take place on the bottom face in a synclinal manner via a chairlike transition state.

Importantly, these structural differences reduce the activation barrier for *Re*-stereofacial addition by 2.15 kcal/mol with respect to the *Si*-stereofacial mode of addition ($\Delta G^{\ddagger}$ = 4.13 (*Re*-addition, (*R*)-**TS1**) vs 6.28 kcal/mol (*Si*-addition, (*S*)-**TS1**), which translates to 98% enantioselectivity, agreeing well with experiment (see the Supporting Information for additional details). The specific origin of this enantiofacial selectivity appears to result

(8) (a) Asami, M.; Mukaiyama, T. *Chem. Lett.* **1980**, 17–20. (b) Meyers, A. I.; Hanagan, M. A.; Trefonas, L. M.; Baker, R. J. *Tetrahedron* **1983**, *39*, 1991–1999. (c) Ohkuma, T.; Kitamura, M.; Noyori, R. *Tetrahedron Lett.* **1990**, *31*, 5509–5512. (d) Watanabe, M.; Hashimoto, N.; Araki, S.; Butsugan, Y. *J. Org. Chem.* **1992**, *57*, 742–744. (e) Zhang, H.; Zhang, S.; Liu, L.; Luo, G.; Duan, W.; Wang, W. *J. Org. Chem.* **2010**, *75*, 368–374. (f) Phan, D. H. T.; Kim, B.; Dong, V. M. *J. Am. Chem. Soc.* **2009**, *131*, 15608–15609. (g) Huang, X.; Pan, X.; Lee, G.; Chen, C. *Adv. Synth. Catal.* **2011**, *353*, 1949–1954.

(9) Mirabdolbaghi, R.; Dudding, T. *Tetrahedron* **2012**, *68*, 1988–1991.

(10) Yus, M.; Gonzalez-Gomez, J. C.; Foubelo, F. *Chem. Rev.* **2011**, *111*, 7774–7854.

(11) (a) Haddad, T. D.; Hirayama, L. C.; Singaram, B. *J. Org. Chem.* **2010**, *75*, 642–649. (b) Hrdina, R.; Valterova, I.; Hodacova, J.; Cisarova, I.; Kotora, M. *Adv. Synth. Catal.* **2007**, *349*, 822–826.

(12) Knepper, K.; Ziegert, R. E.; Brase, S. *Tetrahedron* **2004**, *60*, 8591–8603.

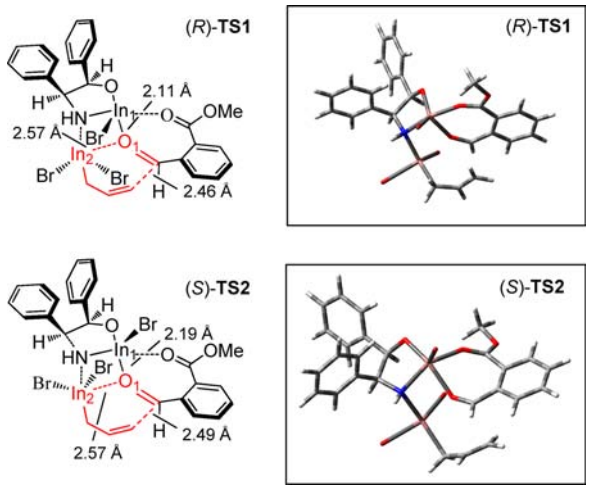

Figure 2. DFT (B3LYP/LanL2DZ)-computed enantioselective transition states (*R*)-**TS1** and (*S*)-**TS2**.

from the presence of a shorter $In_{(1)}\cdots O_{(1)}$ distance in (*R*)-**TS1** (d = 2.11 Å) vs (*S*)-**TS2** (d = 2.19 Å) and increased Pitzer and Baeyer strain in (*S*)-**TS2**. This strain is attributed to the half-chair transition state assembly for allylation in (*S*)-**TS2**, while in (*R*)-**TS1**, allylation proceeds through a less strained, chair-type transition state; see Figure 2 (red atoms).

Charged with this insight as a proof of concept, our efforts then turned toward the experimental realization of our rationally designed $C_{(3)}$-chiral phthalide forming reaction sequence. In this vein, methyl 2-formylbenzoate **1a** (1 equiv) was reacted with allyl bromide (2 equiv), indium powder (2 equiv), (1*R*,2*S*)-(−)-2-amino-1,2-diphenylethanol (2 equiv), and anhydrous pyridine (2 equiv) in THF at −78 °C, which to our delight, as predicted, afforded **2a** in a respectable 80% ee (Scheme 2). Encouraged by this result, a more extensive scan of the substrate scope of this reaction was then explored. Arising from the reaction of electron-rich substrate (methyl 2-formyl-5-methoxybenzoate) **1b**, we isolated phthalide **2b** in ee comparable to that of **2a** (Table 1, entries 1 and 2). Disappointingly, however, the electron-deficient methyl 2-formyl-5-nitrobenzoate substrate **1c** resulted in a dramatic decrease in product ee (Table 1, entry 3). Furthermore, the reactions of the bromo-, carbamate-, and phenyl-5-substituted substrates **1d**−**f** similarly afforded phthalides of moderate ee, which is somewhat interesting considering the electronic and structural differences existing between these substrates (Table 1, entries 4−6).

We then examined the dependence of this reaction on the chain length and steric bulk of the ester group. The resulting trends indicated an increase in ee with diminishing *n*-alkyl carbon chain length (Table 1, entries 7−11). We believe these results may originate from substrate aggregation and potential micelle formation. With respect to changes in steric bulk of the ester group, it was found that increased branching led to erosion of ee. For instance, isopropyl 2-formylbenzoate, **1l**, afforded the product in 64% ee, whereas with *tert*-butyl 2-formylbenzoate, **1m**, no reaction occurred (Table 1, entries 12 and 13). Lastly, to investigate the effect of performing the reaction on a solid support, Merrifield resin bound 2-formylbenzoic acid was then reacted,[12] which disappointingly only afforded racemic phthalide **2a**.

Table 1. Indium-Mediated Enantioselective Allylation[a]/Intramolecular Transestrification of Functionalized Aldehydes

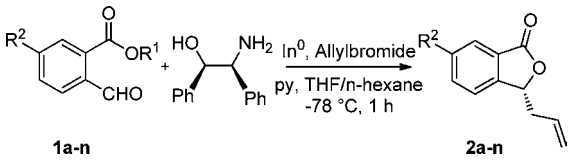

entry		R^1	R^2	product	yield (%)[b]	ee (%)[c]
1	**1a**	CH_3	H	**2a**	77	80
2	**1b**	CH_3	OCH_3	**2b**	67	77
3	**1c**	CH_3	NO_2	**2c**	68	45
4	**1d**	CH_3	Br	**2d**	69	69
5	**1e**	CH_3	isobutyl- CO_2NH	**2e**	65	69
6	**1f**	CH_3	Ph	**2f**	67	68
7	**1g**	C_2H_5	H	**2a**	62	79
8	**1h**	CH_2Ph	H	**2a**	58	76
9	**1i**	C_5H_{11}	H	**2a**	60	71
10	**1j**	C_6H_{13}	H	**2a**	55	65
11	**1k**	$C_{12}H_{25}$	H	**2a**	57	50
12	**1l**	$CH(CH_3)_2$	H	**2a**	78	64
13	**1m**	$C(CH_3)_3$	H	–[d]	0	–[d]
14	**1n**	solid support[e]	H	**2a**	52	0

[a] Allyl bromide, indium powder, (1*R*, 2*S*)-(−)-2-amino-1,2-diphenylethanol, and anhydrous pyridine in THF at −78 °C. [b] Yields of isolated products after flash chromatography. [c] Enantiomeric excess was determined by HPLC analysis. [d] –, not applicable. [e] Merrifield resin was used.

At that stage, the product **2a** obtained from our reaction was assigned as the (*R*)-enantiomer by comparison of its optical rotation with that previously reported by Pedrosa et al. (Supporting Information) which notably was in agreement with the computationally predicted stereochemical outcome. Consequently, to determine if the *ortho*-ester group of our substrates might potentially flip the absolute sense of (*R*)- vs (*S*)-enantioinduction observed in our reaction, we reacted benzaldehyde with allyl bromide under the conditions used throughout this work (Scheme 2). To this end, it was instructively found that we had formed the (*R*)-enantiomer of **6**, as this product had the same direction of optical rotation $[\alpha]^{20}_D = +37$ (c = 1, $CHCl_3$) as previously reported by several groups also as the (*R*)-enantiomer (Supporting Information). As such, this finding was surprising to us considering we had applied the same conditions previously employed by Singaram for the In-mediated allylation of benzaldehyde, with the exception that the enantiomeric antipode of the ligand was used, and yet we observed the same sign of optical rotation reported by Singaram as the (*S*)-enantiomer ($[\alpha]^{25}_D = +48.67$ (c = 0.42, benzene)).[11] Thus, it would

appear based upon these results that the *ortho*-ester group present in our substrates did not flip the absolute sense of (*R*)- vs (*S*)-enantioinduction observed in our reaction.

Scheme 2. Synthesis of (*R*)-1-Phenylbut-3-en-1-ol via an Indium-Mediated Enantioselective Allylation Reaction

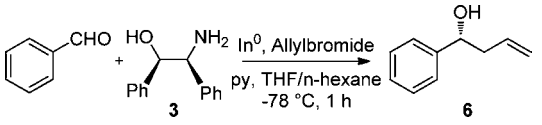

Finally, as a last mechanistic probe, we set out to determine the catalytic role of indium and the in situ generated pyridinium salt (pyr-H^+) on the transesterification step of this reaction. In order to do this, we began by modeling the corresponding transition states for $C_{(3)}$-chiral phthalide forming ring closure, both in the presence ((*R*)-**TS3** and (*S*)-**TS4**) and absence ((*R*)-**TS5** and (S)-**TS6**) of pyr-H^+ and the indium bound complex generated from allylation (see the Supporting Information.). Encouragingly, the results were consistent with our initial mechanistic premise, in that the indium and pyr-H^+ catalyzed transition states were energetically favored over the control transition states in which no catalyst was present. The free energies of activation for transesterification in presence of indium and pyr-H^+ were 5.8 kcal/mol ((*R*)-**TS3**) and 4.5 kcal/mol ((*S*)-**TS4**), while those for the uncatalyzed ring closure were 31.4 and 37.5 kcal/mol for (*R*)-**TS5** and (*S*)-**TS6**, respectively.

Furthermore, to experimentally substantiate this theoretical model, we carried out four separate, representative, intermolecular reactions between 2-propanol and methyl phenylacetate (conditions A−D); see the Supporting Information for details. Under conditions A wherein no indium species or pyr-H^+ was present, product formation was not observed by NMR after 6 h, while in the presence of $InBr_3$ (derived in situ from Br_2 and In) product formation was observed and the reaction had gone to ~40% completion after 6 h (conditions B). Similarly, when pyridium salt pyr-H^+ (conditions C) was employed as the sole catalyst, a marked product formation was again observed. However, unfortunately when the reaction was performed in the dual catalytic presence of In/Br_2 and pyr-H^+, the formation of an intractable mixture of byproduct resulted (conditions D). Given these trends, we believe that further investigation is warranted to better understand the outcome of this reaction under the catalytic action of both In/Br_2 and pyr-H^+ (i.e., conditions D).

Taken together, we have disclosed here an In-promoted one-pot allylation/intramolecular transesterification sequence and accompanying DFT rationale of stereoselection that provides enantioenriched $C_{(3)}$-functionalized chiral phthalides (**2a**−**l**). Notably, to the best of our knowledge, this work presents the first example of a DFT-drafted stereochemical model for rationalizing the observed enantioselectivity of a reaction. Moreover, an interesting dependence of the ee of this reaction upon the steric size and chain length of the ester appendage undergoing transesterification during this reaction dynamic was revealed. Ongoing efforts in our laboratory focus on the expansion and integrated use of this protocol in total synthesis.

Acknowledgment. We are grateful to the Natural Sciences and Engineering Research Council of Canada (NSERC) for funding of this research. We thank Dr. Costa Metallinos and Joshni John of Brock University for use of equipment.

Supporting Information Available. Experimental procedures, full spectroscopic data for all new compounds, and computational details. This material is available free of charge via the Internet at http://pubs.acs.org.

The authors declare no competing financial interest.